

Sensitivity analysis of kinetic, thermodynamic, and transport parameters in HMX (1,3,5,7-tetranitro-1,3,5,7-tetrazocane) combustion modeling

Jie-Yao Lyu^a, Qiren Zhu^a, Geng Xu^b, Fangmian Dong^b, Xin Wang^b, Song He^c, Xinyi Zhou^a, Yichen

Zong^{a,c}, Markus Kraft^{d,e}, Yang Li^{b,*}, Wenming Yang^{a,*}

a. Department of Mechanical Engineering, College of Design and Engineering, National University of Singapore, 9 Engineering Drive 1, Singapore, 117575, Singapore.

b. Science and Technology on Combustion, Internal Flow and Thermo-structure Laboratory, Northwestern Polytechnical University, Xi'an 710072, China.

c. School of Energy and Electromechanical Engineering, Hunan University of Humanities, Science and Technology, China.

d. Cambridge Centre for Advanced Research and Education in Singapore, Singapore.

e. Department of Chemical Engineering and Biotechnology, University of Cambridge, United Kingdom.

Abstract: Chemical kinetic mechanisms are crucial for modeling the combustion processes of solid propellants, but the specific impacts of these mechanism's parameters on combustion have not been fully assessed. This study conducted a comprehensive sensitivity analysis on kinetics, thermodynamics, and transport parameters affecting solid propellant mechanisms, exemplified with HMX as a case study. A one-dimensional steady-state numerical model incorporating gas and liquid phase mechanisms of HMX was developed and validated against experimental data. This model enables a thorough sensitivity analysis to evaluate the influence of various parameters, including the reaction constant (k) of each elementary reaction, enthalpy of formation (h_f), entropy (s), heat capacity (c_p), collision diameter (σ), and potential well-depth (ε) of each species, on key combustion characteristics over a wide range of pressure. The analysis revealed that gas kinetics predominantly govern the HMX combustion compared to liquid kinetics, particularly at high pressures. Notably, the decomposition reactions of $\text{H}_2\text{C}(\text{NO})_2$ and N_2O in the gas phase were identified as highly sensitive reactions that control the r and the pressure exponent of HMX. By calculating the normalized sensitivity coefficients of all parameters, the c_p values of small gaseous molecules were found to be the most significant factors affecting combustion, indicating a role played by the thermodynamic properties of small species. This research could enhance our understanding of HMX combustion mechanisms and underscore critical areas for future development and refinement of detailed kinetic mechanisms of solid propellants.

Keywords: Sensitivity analysis; Solid propellant; HMX; Combustion modeling; Kinetic mechanism.

* Corresponding authors E-mail: mpeywm@nus.edu.sg (Yang Wenming); yang.li@nwpu.edu.cn (Li Yang).

(1) Novelty and significance

The novelty of this research lies in conducting a comprehensive sensitivity analysis on the mechanism parameters of HMX to assess their impacts on combustion characteristics such as burning rate, thereby addressing a crucial question: how do these parameters influence the combustion process of HMX? Despite recent extensive research into the development of detailed kinetic mechanisms for solid propellant ingredients, such as RDX (*Combust. Flame*, 2022: 112220), HMX (*Combust. Flame*, 2024: 113181), and AP (*Combust. Flame*, 2023: 112891), the nuanced effects of kinetic, thermodynamic, and transport parameters on their combustion have been underexplored. Our findings illuminated the critical role of the heat capacity of small molecules and elucidate the significance of each parameter, which could enhance our understanding of solid propellant combustion. This research not only refines the existing kinetic mechanism but also guides future advancements in the development and reduction of mechanisms for other solid propellants.

(2) Author Contributions

- Jie-Yao Lyu's contributions: research conduction, coding, data analysis, writing.
- Qiren Zhu's contribution: data analysis.
- Geng Xu's contribution: coding.
- Fangmian Dong's contribution: coding.
- Xin Wang's contribution: data analysis.
- Song He's contribution: revision.
- Xinyi Zhou's contribution: data analysis, revision.
- Yichen Zong's contribution: computational sources, revision.
- Markus Kraft's contribution: computational sources, conceptualization.
- Yang Li's contribution: conceptualization, revision, supervision.
- Wenming Yang's contribution: computational sources, conceptualization, revision, supervision.

1. Introduction

Solid propellants are the main source of energy and working medium of the solid rocket motor, greatly determining the propulsion performance of aerospace vehicles [1][2][3]. However, the complexity and hostile operating environment of solid propellants limit their comprehensive experimental testing for key combustion characteristics like burning rate (r) [4], flame temperature [5], and species evolution [6]. Therefore, it is essential to couple the chemical kinetic mechanisms of corresponding formulation with numerical models to simulate the combustion of solid propellants, to deepen our understanding of their combustion processes.

In the past two decades, a lot of detailed kinetic mechanisms of solid propellants have been proposed, for instance, detailed gas mechanisms on AP with 36 species and 205 reactions by Bernigaud et. al. [7], on nitramines (RDX and HMX) with 89 species and 462 reactions by Chakraborty et al. [8], on ammonium dinitramide (AND) with 32 species and 152 reactions by Park et al. [9], on nitroglycerin (NG) with 74 species and 1011 reactions by Glorian et al. [10], on nitrocellulose (NC) with 62 species and 803 reactions by Ehrhardt et al. [11]. In addition, newly developed mechanisms of novel energetic materials (such as 1,1-diamino-2,2-dinitroethylene (FOX-7) [12][13][14][15], 2,4,6,8,10,12-hexanitro-2,4,6,8,10,12-hexaazaisowurtzitane (CL-20) [16][17][18]) are still being investigated, and existing mechanisms are continuously refined (e.g. ammonium nitrate (AN) [19], RDX [20][21][22], HMX [23]). Besides, to replace simple and crude global kinetics of the liquid phase, liquid detailed mechanisms have been developed to describe the decomposition chemistry, such as liquid mechanism on AP with 85 reactions by Zhu et al. [24], on RDX with 53 species and 56 reactions by Khichar et. al. [25], on HMX with 109 species and 157 reactions by Patidar et al. [26]. Despite these advancements in detailed kinetic mechanisms, the influence of these mechanism parameters on the combustion process of solid propellants remains unclear.

Sensitivity analysis is widely used in combustion science for exploring the relationships between input parameters and outputs, and this approach has been proven effective in improving existing mechanisms of hydrocarbons or oxygenated hydrocarbons, as well as surrogate fuels, through identifying parameters requiring further refinement by experiments and quantum chemical calculations [27][28]. The 0-dimensional homogeneous reactor and one-dimensional laminar flame have been widely employed for sensitivity analysis of kinetic mechanisms. Besides, the sensitivity analysis could also deepen our understanding of the combustion processes as well as the couplings between these processes [29].

1
2
3
4
5
6
7
8
9
10
11
12
13
14
15
16
17
18
19
20
21
22
23
24
25
26
27
28
29
30
31
32
33
34
35
36
37
38
39
40
41
42
43
44
45
46
47
48
49
50
51
52
53
54
55
56
57
58
59
60
61
62
63
64
65

However, especially when compared with hydrocarbon fuels, the kinetic mechanism parameters of solid propellants lack comprehensive sensitivity analysis. The sensitivity analysis using established models for solid propellant ingredient combustion allows a natural link between experimental and modeling efforts and can be used to design experiments and to identify key reactions and species that require further theoretical study [30]. Therefore, a proper numerical model that couples detailed kinetic mechanisms to model concerned characteristics of solid propellant, such as burning rate, is required for performing further sensitivity analysis.

The numerical models of solid propellant combustion have been developed tremendously in the past half century, and relative advances were well-reviewed with the focus on homogeneous models by Beckstead et al. [30], and heterogeneous models by Jackson [31]. Among these models, the one-dimensional steady-state combustion model coupling with liquid and gas phase mechanisms is suitable for performing sensitivity analysis of mechanism parameters, because of its universality and computational efficiency. The first combustion model of nitramines coupled with detailed kinetic mechanisms was attributed to Melius [32][33] in 1990, where they analyzed the sensitivity of gas kinetics to the r at 1 atm using the brute-force method. In 1995, Liao and Yang [34] investigated the differences in temperature and species concentrations by using Yetter's [35] and Melius's [32][33] mechanism of RDX at 1 atm. Subsequently, Davidson and Beckstead [36] conducted a sensitivity analysis on the parameters of a nitramine combustion model, including heat feedback, vapor pressure, thermal conductivities, heat capacities, melting heat, and melting temperature, but the sensitivity of mechanism parameters remained unexplored. Kim et al. [37] proposed a GAP/HMX combustion model in 2002, and they performed a parametric study on the effect of reaction rates of R1 and R2 of a condensed-phase mechanism (19 species and 10 reactions) 1 atm. In 2004, Miller and Anderson [38] systematically calculated the normalized sensitivities of the temperature of the second grid above the burning surface to the gas kinetics in a nitrate-ester propellant's flame, as it was assumed that the temperature of the second grid is the most sensitive determinant of the computed heat feedback to the surface, and the heat feedback will determine the r of the propellants. In 2009, by adopting the same methodology as [38], Anderson and Corner [39] compared two different RDX combustion models (Yetter's [40] and CTM's model [8][41]) and calculated the sensitivity coefficients of their gas kinetics. It was found that small molecule chemistry, e.g., $\text{HNC} + \text{OH} = \text{HNCO} + \text{H}$, is critical for the combustion of RDX. Therefore, they believed that if the small molecule chemistry is correct, the combustion characteristics are likely to be correctly

1 predicted even if the initial RDX reactions are wrong. The same method was employed by Patidar and
2 Thynell et al. [42] to quantify the sensitivity of the transport parameters to the combustion performance
3 of RDX in 2019. The results suggested that the σ of RDX, H, and H₂O were more sensitive than the gas
4 kinetics at a 1-10 atm, highlighting the importance of mechanism parameters beyond the kinetics.
5
6 However, these above-mentioned works have not evaluated the effect of thermodynamics to form a
7 systematic evaluation of all mechanism parameters. Furthermore, except for Melius [32], other works
8 did not link the mechanism parameters with concerned combustion characteristics directly when
9 performing the sensitivity analysis.
10

11
12 As such, in this study, a comprehensive sensitivity analysis of kinetic, thermodynamic, and transport
13 parameters is performed for the combustion of HMX, which is also an important ingredient of solid
14 propellant as RDX and whose sensitivity has not been assessed yet. Similarly, a one-dimensional steady-
15 state combustion model with three phases is employed, coupled with detailed kinetic mechanisms of
16 HMX in the liquid and gas phases. The model is validated against experimental results over a wide
17 pressure range. Then, the validated model is employed to analyze the sensitivity of mechanism
18 parameters, and the normalized sensitivity coefficients are calculated to compare parameters across
19 groups. At last, the significance of evolved parameters is identified and discussed. Such analysis can
20 provide more insights into solid propellant combustion processes, guide us to improve the accuracy of
21 existing kinetic mechanisms by further calculations or experiments, and highlight the focus of future
22 research on developing, optimizing, and simplifying the detailed kinetic mechanisms of solid propellants.
23
24

25 26 27 28 29 30 31 32 33 34 35 36 37 38 39 **2. Methodology**

40 41 **2.1. Numerical model for HMX combustion**

42
43 To conduct the sensitivity analysis of mechanism parameters, a one-dimensional steady-state
44 numerical model for solid propellant combustion has been employed, consistent with previous studies
45 [30, 32-34][43][44]. As depicted in Fig. 1, the model is divided into three phases: solid, liquid, and gas.
46
47 The reference frame is anchored at the burning surface (liquid-gas interface), with a semi-infinte piece
48 of HMX modeled for the combustion process. The detailed kinetic mechanisms are incorporated into the
49 liquid and gas phases, and the phase transformation of HMX happens in the solid phase.
50
51
52
53
54
55
56
57
58
59
60
61
62
63
64
65

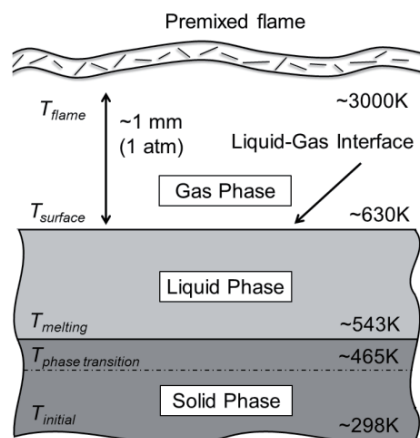


Fig. 1. Schematic chart of the one-dimensional steady-state model with three phases for HMX combustion.

2.1.1 Solid phase

It is reasonably assumed that no reaction occurs in the solid phase due to the low-temperature condition and short residence time, where only heat conduction exists in this phase. The energy equation is as:

$$\frac{d}{dx} \left(k \frac{dT}{dx} \right) = \dot{m}'' c_p \frac{dT}{dx} \quad (1)$$

where x is the axial distance vertically from the burning surface, $x = 0$ refers to the burning surface, k is the thermal conductivity of the solid phase, T is the temperature, \dot{m}'' is the mass flux rate, and c_p is the heat capacity of the solid phase. For the solid phase of HMX combustion modeling, the β - δ phase transformation is considered to occur at 465 K [45] with the endothermy of 2.35 kcal/mol ($\Delta H_{\beta-\delta}$) [30]. Thus, the whole solid domine is divided into two regions, the β -HMX region and the δ -HMX region. The Eq. (1) is integrated numerically as a combination of two first-order ODEs along all two regions as below:

$$\begin{cases} \frac{dk\tau}{dx} = \dot{m}'' c_p \tau \\ \frac{dT}{dx} = \tau \end{cases} \quad (2)$$

The boundary conditions of the β -HMX region are the room temperature (lower boundary) and the phase transformation temperature (upper boundary), respectively. The boundary conditions of the δ -HMX region are as below:

$$T = 465 \text{ K} \quad \text{and} \quad \frac{dT}{dx} = \frac{\dot{m}''}{k} \left[\Delta H_{\beta-\delta} + \int_{298 \text{ K}}^{465 \text{ K}} c_p dT \right] \quad \text{at} \quad x = x_{\beta-\delta} \quad (3)$$

The energy equations Eq. (2) of β -HMX and δ -HMX regions are solved using the DOVDE stiff ODE solver along the x axial. The solution terminates when the temperature reaches the melting point of

1 the melting temperature of the HMX (543 K), which is assumed to be constant and independent of the
2 pressure.

3 4 **2.1.2 Liquid phase**

5
6 The liquid phase is described as a one-dimensional reactor to present the initial decomposition of
7 HMX after the HMX melts, consistent with the model of Prasad et al. [30, 40]. The diffusion process in
8 this phase is ignored, since the liquid diffusion is much slower than that of the gas phase, and the thickness
9 of this zone is thin relative to the burning surface regression [30, 32, 43, 44]. The conservation equations
10 of species and energy are as follows:

$$11 \quad \dot{m}'' \frac{dY_i}{dx} = \dot{\omega}_i W_i \quad (4)$$

$$12 \quad \dot{m}'' c_p \frac{dT}{dx} = \frac{d}{dx} \left(k \frac{dT}{dx} \right) - \sum_{i=1}^n \dot{\omega}_i h_i W_i \quad (5)$$

13
14 where Y_i , $\dot{\omega}$, h_i , and W_i are the mass fraction, molar production rate, enthalpy, and molecular
15 weight of the i th species involved in the liquid mechanism, respectively. The boundary condition of
16 species equation is that $Y=1$ for HMX and 0 for other species. The boundary condition of temperature is
17 the melting temperature at the lower boundary, and the temperature gradient at the solid-liquid interface
18 (melting point) is obtained from the solved dT/dx at the upper boundary of the solid phase combining the
19 melting process, with ΔH_{melt} of 16.7 kcal/mol for HMX [30]:

$$20 \quad T = 543 \text{ K} \quad \text{and} \quad \frac{dT}{dx} = \frac{\dot{m}''}{k} \left[\Delta H_{\beta-\delta} + \Delta H_{melt} + \int_{298 \text{ K}}^{543 \text{ K}} c_p dT \right] \quad \text{at} \quad x = x_{melting \text{ point}} \quad (6)$$

21
22 The conservation equation of the energy is also treated as a combination of two first-order ODEs as
23 solid phase equation, and then both species and energy equations are solved using the DOVDE stiff ODE
24 solver along the x axial until the T reaches the experimentally measured burning surface temperature.
25 After the temperature of the liquid phase reaches the T_s , the decomposition products together with
26 unreacted HMX are considered to vaporize to be corresponding gas species for further flame modeling.
27 Note that for the one-dimensional steady-state model for solid propellant ingredients combustion, the
28 continuity equation $d\dot{m}/dx = 0$ is applied across all three phases. The \dot{m}'' is unknown that is to be
29 determined as an eigenvalue in this problem. To make this eigenvalue problem well-posed, an additional
30 boundary must be given; herein, the dependence of the burning surface temperature (T_s) on the \dot{m}'' is
31 pointed out. This approach is expressed as Arrhenius-like pyrolysis law, consistent with the that employed
32 in [30][43][46]:

$$33 \quad \dot{m}'' = A_s \exp(-E_s/RT_s) \quad (7)$$

1 where E_s is the surface activation energy, that is a characteristic of the family of chemicals the
2 ingredient belongs to, and A_s is a constant to be derived from the experimental results. In this HMX
3 model, E_s and A_s were fitted as $23250.0 \text{ cal}\cdot\text{mol}^{-1}$ and $7.0\text{E}6 \text{ g}\cdot\text{cm}^{-2}\cdot\text{s}^{-1}$, respectively, derived from
4 experimental results in [47].
5
6

7 8 **2.1.3 Gas phase** 9

10 The gas phase is described as a one-dimensional burner flame, and the burner-stabilized model of
11 the open-source chemical kinetics software package CANTERA [48] was employed for solving the gas-
12 phase domain, by ignoring the macroscopic convection effect and pressure change in every iteration. The
13 compressibility is described by Eq. (8); The mass conservation and diffusion flow of each gas-phase
14 species is described by Eq. (9); The energy equation considers the combined contribution of heat
15 conduction, chemical reaction, and gas diffusion, as Eq. (10):
16
17
18
19
20
21

$$22 \quad \rho RT = p\bar{W} \quad (8)$$

$$23 \quad \dot{m}'' \frac{dY_i}{dx} + \frac{d}{dx}(\rho Y_i V_i) = \dot{\omega}_i W_i \quad (9)$$

$$24 \quad \dot{m}'' c_p \frac{dT}{dx} = \frac{d}{dx} \left(k \frac{dT}{dx} \right) - \sum_{i=1}^n \dot{\omega}_i h_i W_i - \sum_{i=1}^n \rho Y_i V_i c_{p,i} \frac{dT}{dx} \quad (10)$$

25 where ρ is the density, R is the universal gas constant, p is the pressure, \bar{W} is the mean molecular
26 weight, V_i and $c_{p,i}$ are the diffusion and specific heat capacity of the i th species. The far-field conditions
27 of this phase require the gradients of flow properties to be zero. By inputting an initial guess value of
28 \dot{m}'' , the model started to iterate between the gas and liquid layer, until the energy inflow from the gas
29 phase to the burning surface equals to the net energy outflow from the surface to the liquid phase. The
30 solved \dot{m}'' is given by Eq. (7) when the whole model is solved when energy balance is achieved.
31
32
33
34
35
36
37
38
39
40
41

42 **2.2. Detailed kinetic mechanisms** 43

44 To exemplify the sensitivity analysis, a classical detailed kinetic mechanism of HMX combustion
45 developed by Chakraborty et al. [8][49] with further update [50] with 81 species and 278 reactions was
46 used in the present study. The liquid thermal decomposition was described by a detailed reaction
47 mechanism with 107 species and 157 reactions developed by Patidar et al. [26, 50]. All mechanisms used
48 in this study are available in the Supplementary Materials.
49
50
51
52
53

54 **2.3. Sensitivity analysis** 55

56 In this study, the local sensitivity analysis based on the brute-force approach was adopted to quantify
57 the significance of kinetic, thermodynamic, and transport parameters under 5 atm, 100 atm, and 200 atm,
58
59
60

1
2
3
4
5
6
7
8
9
10
11
12
13
14
15
16
17
18
19
20
21
22
23
24
25
26
27
28
29
30
31
32
33
34
35
36
37
38
39
40
41
42
43
44
45
46
47
48
49
50
51
52
53
54
55
56
57
58
59
60
61
62
63
64
65

to represent low, medium, and high pressures, respectively. For simplicity, the r is chosen as the representative of the combustion characteristic for clarity. To compare the significance across the groups, the normalized sensitivity coefficients were calculated for each mechanism parameter. The normalized sensitivity coefficient targets at pressure exponent and flame temperature were also calculated. All raw calculation results are available in the Supplementary Materials.

2.3.1 Kinetic parameters

The reaction rate constant (k) of each elementary reaction was multiplied and divided by a factor of 2 to obtain the corresponding modified burning rate, r_{mod} . The unmodified burning rates were recorded as r_0 . The normalized sensitivity coefficient was calculated as follows.

$$SC_k^r = \frac{r_{mod,1} - r_{mod,2}}{2k - 0.5k} \frac{k}{r_0} \quad (11)$$

2.3.2 Thermodynamic parameters

The thermodynamic parameters of each species include heat capacity (c_p), enthalpy of formation (h_f), and standard entropy (s), fitted by the NASA polynomials with two sets of coefficients a_i ($i = 1, 2, \dots, 7$) to describe the high- and low-temperature intervals. To better understand the significance of each kind of thermodynamic parameter, the sensitivity analysis was conducted concerning the c_p , h , and s , instead of a_i . The normalized sensitivity coefficients to the r were defined analogously as Lehn and Lemke et al. [28][51], and it was elaborated here briefly.

$$SC_{c_p}^r = \frac{1}{SAF-1} \frac{r_{mod}-r_0}{r_0} \quad (12)$$

$$SC_{h_f}^r = \frac{r_{mod}-r_0}{r_0} \frac{R \cdot 298K}{\delta \Delta h_f} \quad (13)$$

$$SC_s^r = \frac{r_{mod}-r_0}{r_0} \frac{R}{\delta s} \quad (14)$$

In practice, the modified c_p was obtained by multiplying the a_i ($i = 1, 2, \dots, 5$) with a sensitivity analysis factor (SAF), which was meticulously chosen as 1.2 in this study. Since $SC_{h_f}^r$ is desired for h_f only, the other two coefficients a_6 and a_7 were changed correspondingly to ensure that h and s were maintained at 298K. The $\delta \Delta h_f$ was chosen to be $R \cdot 1000K$, obtained by increasing a_6 without touching other coefficients. The choice of using this delta value is also explained in the Supplementary Materials. Similarly, the δs was set as R by increasing a_7 alone, $R = 1.987 \text{ cal} \cdot \text{K}^{-1} \cdot \text{mol}^{-1}$. In our pilot study, different SAF values (1.02, 1.10, and 1.20) has been tested, and 1.20 was chosen to calculate the normalized sensitivity coefficients to minimum disturbance from the convergence error of the numerical

1
2
3
4
5
6
7
8
9
10
11
12
13
14
15
16
17
18
19
20
21
22
23
24
25
26
27
28
29
30
31
32
33
34
35
36
37
38
39
40
41
42
43
44
45
46
47
48
49
50
51
52
53
54
55
56
57
58
59
60
61
62
63
64
65

model. Similarly, different $\delta\Delta h_f$ and δs have been investigated and the results can be found in the Supplementary Materials

2.3.3. Transport parameters

Among all tabulated inputs of transportation, the Lennard-Jones parameters, namely, potential well-depth (ϵ), and collision diameter (σ), were selected for analysis in this study, because of their significance compared with dipole moment, polarizability, and rotational relaxation collision number [52]. They were multiplied by a factor of 2, and the corresponding output was recorded. Since mass diffusion was ignored in the liquid phase, only the transport parameters in the gas phase were considered here. The normalized coefficients were calculated below.

$$SC_{\epsilon}^r = \frac{r_{mod}-r_0}{2\epsilon-\epsilon} \frac{\epsilon}{r_0} \quad (14)$$

$$SC_{\sigma}^r = \frac{r_{mod}-r_0}{2\sigma-\sigma} \frac{\sigma}{r_0} \quad (15)$$

3. Results and discussions

3.1. Model validation

Before sensitivity analysis, it is necessary to validate the model coupled with detailed mechanisms of HMX by comparing its predicted results against experimental results, including r under different pressures, flame temperatures, and species evolutions. The dependence of r of HMX combustion on pressures from 1 to 200 atm is depicted in Fig. 2.

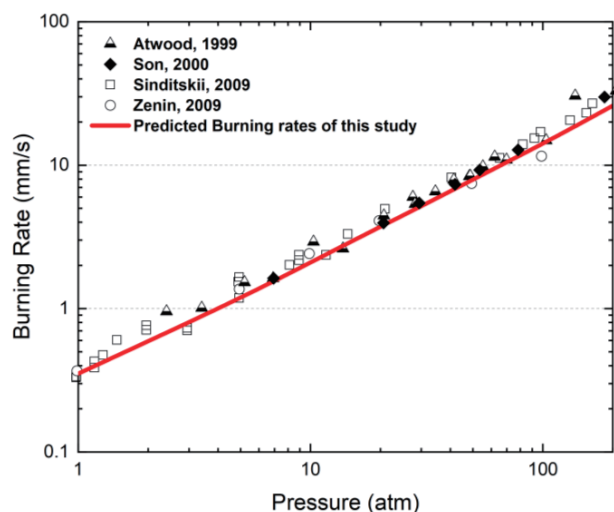


Fig. 2. Predicted burning rates (line) and experimental data (symbols) [53][54][55][56] under 1-200 atm.

A satisfactory agreement was obtained between predicted results and experimental data. The pressure exponent (n) of HMX was fitted to be 0.85, which is also equivalent to the experimental result

1
2
3
4
5
6
7
8
9
10
11
12
13
14
15
16
17
18
19
20
21
22
23
24
25
26
27
28
29
30
31
32
33
34
35
36
37
38
39
40
41
42
43
44
45
46
47
48
49
50
51
52
53
54
55
56
57
58
59
60
61
62
63
64
65

from Son et al. [53]. The predicted temperature profiles of gas, liquid, and solid phases under 1 atm, 5 atm, 20 atm, and 70 atm along the HMX propellant axial are presented in Fig. 2. Since the flame structure of solid propellant is hard to measure with an ideal accuracy experimentally, the predicted results were validated against the adiabatic flame temperatures calculated by NASA CEA program, and a similar trends were obtained with that of Liao and Yang's regarding RDX [34] and Prasad et al. [44] of HMX.

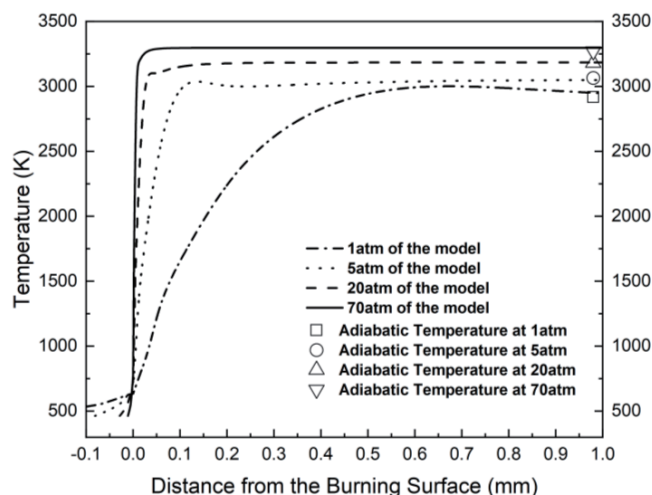


Fig. 3. Predicted temperature profiles of HMX combustion under 1 atm, 5 atm, 20 atm, and 70 atm.

The species mole fraction profiles obtained by this model are compared with experimental results from Paletsky et al. [57] (Fig. 4), where the results of the present model reasonably agree with the experiments. We acknowledge the discrepancy in species profiles near the burning surface ($x < 0.5$ mm), where numerical results show faster evolutions than the experimental data. In specific, the peaks of NO and HCN were calculated to locate around 0.25 mm over the burning surface, while no corresponding peak was observed in experimental results. This discrepancy likely arises from the limitations of the mass spectrometry technique used in the experimental measurements, which struggles with precision and timely response at such small spatial and time scales and high temperatures. Additionally, locating the exact burning surface is challenging due to uneven regression across the section. A faster consumption of nitramines is also obtained in other modeling results [32, 34, 39]. In this study, the reasonable agreement was achieved for evolution trends of species and mole concentrations in the final flame. Therefore, it is believed that the employed model can represent the combustion characteristics of HMX, indicating its capability for performing further sensitivity analysis.

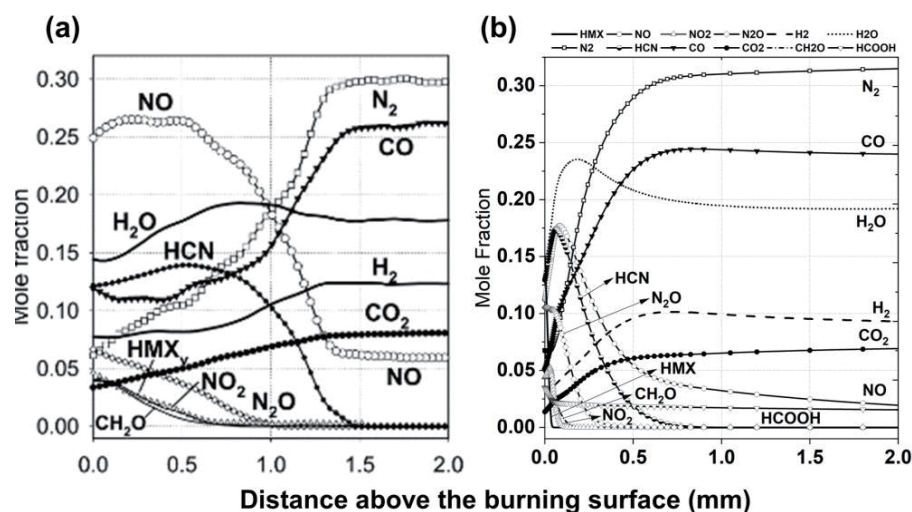


Fig. 4. Averaged and smoothed species profiles of HMX flame by experiments under atmospheric conditions (a, [57]) and predicted species profiles of HMX under 1 atm (b).

3.2. Sensitivity analysis of kinetics

The sensitivity of gas and liquid kinetics to the burning rate (r) can be determined by calculating the normalized sensitivity coefficients of k , and the top 10 sensitive elementary reactions (with the highest sum of absolute sc under all pressures) are summarized in Fig 5. In the gas phase, the reactions involving H_2CNNO_2 , $HNCO$, and N_2O are most significant. Specifically, the decomposition of N_2O into N_2 and an O radical is identified as one of the most sensitive reactions at 5 atm (low pressure), consistent with Melius's findings in an RDX flame at 1 atm [32], and Anderson and Corner's results in an RDX flame at 0.5 atm [39]. However, its significance diminishes at higher pressures. Of all gas phase reactions, the decomposition reaction of H_2CNNO_2 to form H_2CN and NO_2 (R220) was found to be the most sensitive one, with sc' of -0.13, -0.08, and -0.07, at 5 atm, 100 atm, and 200 atm, respectively. The top 10 sensitive reactions in the gas phase under different pressures can be found in Tab 1. After a more detailed exploration of the initial decomposition processes of nitramines by Prasad et al. [40], Yetter et al. [35], Chakraborty et al. [8, 41, 49], and Patidar et al. [50], the significance of H_2CNNO_2 was found to be more evident. The H_2CNNO_2 serves as the primary initial decomposition intermediate of ring-open reactions of RDX and HMX, and its reactions produce mostly NO_2 and significant N_2O . It could be concluded that the ring-open kinetics are vital for determining the whole combustion process of HMX propellant. However, the reactions directly connected with the initial HMX decomposition are much less sensitive.

1
2
3
4
5
6
7
8
9
10
11
12
13
14
15
16
17
18
19
20
21
22
23
24
25
26
27
28
29
30
31
32
33
34
35
36
37
38
39
40
41
42
43
44
45
46
47
48
49
50
51
52
53
54
55
56
57
58
59
60
61
62
63
64
65

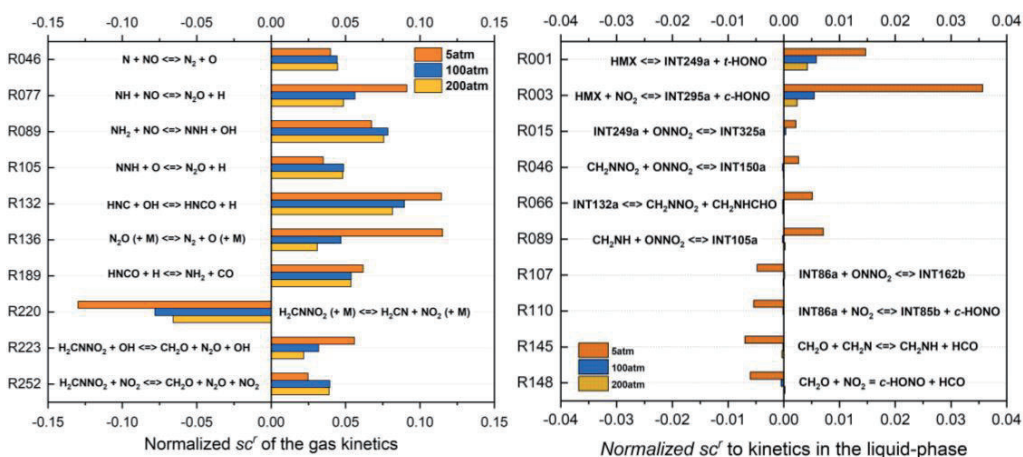


Fig. 5. Normalized sensitivity coefficients of gas and liquid kinetics to r under 5 atm, 100 atm, and 200 atm.

For liquid kinetics, the initial decomposition reaction of HMX (R1) and H-atom abstraction of HMX by NO_2 (R3) are the most two sensitive reactions. However, the absolute sc' of liquid kinetics are much lower than those of gas ones, indicating a stronger effect of gas kinetics for controlling the flame of HMX. It is believed that the low decomposition ratio of nitramines in the liquid is responsible for this discrepancy in the sensitivity. The decomposition ratio in the liquid phase was calculated as 4.9%, 0.9%, and 0.4% at 5 atm, 100 atm, and 200 atm, respectively, which is consistent with the findings reported regarding RDX and HMX in [32].

Tab. 1. Top 10 sensitive elementary reactions in the gas phase with the corresponding sc' at 5, 100, and 200 atm.

5 atm			100 atm			200 atm		
R220	$\text{H}_2\text{CNNO}_2 (+ \text{M})$	-	R132	$\text{HNC} + \text{OH} \rightleftharpoons$	0.09	R132	$\text{HNC} + \text{OH} \rightleftharpoons$	0.08
	$\rightleftharpoons \text{H}_2\text{CN} + \text{NO}_2$	0.14		$\text{HNCO} + \text{H}$			$\text{HNCO} + \text{H}$	
	(+ M)							
R136	$\text{N}_2\text{O} (+ \text{M}) \rightleftharpoons \text{N}_2$	0.12	R089	$\text{NH}_2 + \text{NO} \rightleftharpoons$	0.08	R089	$\text{NH}_2 + \text{NO} \rightleftharpoons$	0.08
	+ O (+ M)			$\text{NNH} + \text{OH}$			$\text{NNH} + \text{OH}$	
R132	$\text{HNC} + \text{OH} \rightleftharpoons$	0.12	R220	$\text{H}_2\text{CNNO}_2 (+ \text{M})$	-	R220	$\text{H}_2\text{CNNO}_2 (+ \text{M})$	-
	$\text{HNCO} + \text{H}$			$\rightleftharpoons \text{H}_2\text{CN} + \text{NO}_2$	0.08		$\rightleftharpoons \text{H}_2\text{CN} +$	0.07
				(+ M)			$\text{NO}_2 (+ \text{M})$	
R077	$\text{NH} + \text{NO} \rightleftharpoons \text{N}_2\text{O}$	0.10	R077	$\text{NH} + \text{NO} \rightleftharpoons \text{N}_2\text{O}$	0.06	R189	$\text{HNCO} + \text{H} \rightleftharpoons$	0.05
	+ H			+ H			$\text{NH}_2 + \text{CO}$	
R089	$\text{NH}_2 + \text{NO} \rightleftharpoons$	0.07	R189	$\text{HNCO} + \text{H} \rightleftharpoons$	0.05	R077	$\text{NH} + \text{NO} \rightleftharpoons$	0.05
	$\text{NNH} + \text{OH}$			$\text{NH}_2 + \text{CO}$			$\text{N}_2\text{O} + \text{H}$	
R189	$\text{HNCO} + \text{H} \rightleftharpoons$	0.07	R105	$\text{NNH} + \text{O} \rightleftharpoons \text{N}_2\text{O}$	0.05	R105	$\text{NNH} + \text{O} \rightleftharpoons$	0.05

1
2
3
4
5
6
7
8
9
10
11
12
13
14
15
16
17
18
19
20
21
22
23
24
25
26
27
28
29
30
31
32
33
34
35
36
37
38
39
40
41
42
43
44
45
46
47
48
49
50
51
52
53
54
55
56
57
58
59
60
61
62
63
64
65

	NH ₂ + CO			+ H			N ₂ O + H	
R223	H ₂ CNNO ₂ + OH	0.06	R136	N ₂ O (+ M) <=> N ₂	0.05	R046	N + NO <=> N ₂	0.04
	<=> CH ₂ O + N ₂ O +			+ O (+ M)			+ O	
	OH							
R140	N ₂ O + H <=> N ₂ +	-	R046	N + NO <=> N ₂ +	0.04	R252	H ₂ CNNO ₂ + NO ₂	0.04
	OH	0.06		O			<=> CH ₂ O +	
							N ₂ O + NO ₂	
R248	H ₂ CNNO ₂ <=>	0.05	R252	H ₂ CNNO ₂ + NO ₂	0.04	R163	NCO + M <=> N	0.03
	INT74a			<=> CH ₂ O + N ₂ O +			+ CO + M	
				NO ₂				
R046	N + NO <=> N ₂ +	0.04	R223	H ₂ CNNO ₂ + OH	0.03	R136	N ₂ O (+ M) <=>	0.03
	O			<=> CH ₂ O + N ₂ O +			N ₂ + O (+ M)	
				OH				

To better understand the role that the kinetics play in the pressure dependence of HMX combustion, the normalized sensitivity coefficients to the pressure exponent (n) were also calculated (Fig. 6). The n is one of the most concerning characteristics of solid propellant combustion. It could be fitted by the Vieille law, $r = ap^n$, where p is the ambient pressure. Among gas kinetics, the decomposition of N₂O (R136) has the highest absolute value of sc^n (-0.027). It indicates that the n of HMX could be suppressed efficiently by enhancing this elementary reaction. Similarly, the sensitivity coefficients of liquid reactions were calculated and their sc^n values are smaller than 0.007. All calculation results can be seen in the Supplementary Information.

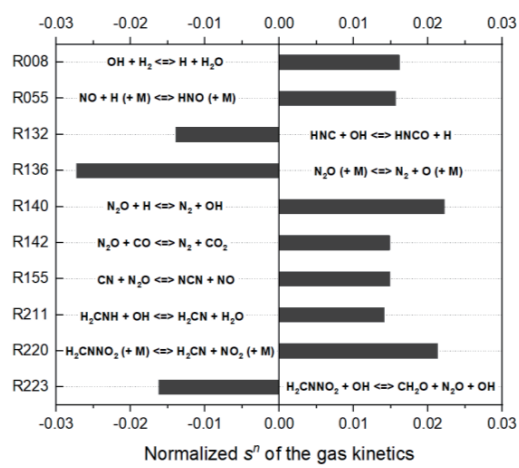


Fig. 6. Normalized Sensitivity coefficients of gas kinetics to n .

To find out the inherent connectivity between the sensitivity of HMX propellant combustion and gaseous HMX ignition, the normalized sensitivity coefficients of gas kinetics to the OH radical concentration were also calculated by using the 0-dimensional homogeneous reactor with 1500 K under different pressures, by the ChemkinPro program [58]. The top 10 sensitive reactions are displayed in Fig. 7. It can be found those reactions sensitive to the ignition of HMX are inequivalent to the reactions that are sensitive to the HMX propellant combustion. For instance, only four reactions among the top 10 sensitive reactions in Fig. 7, namely, R105, R220, R223, and R252, are ranked in Fig. 5. It demonstrates that the sensitivity analysis approach of solid propellant combustion distinguishes with approaches of conventional hydrocarbon fuels because of their different combustion characteristics. Moreover, the mechanism reduction based on the sensitivity analysis becomes inappropriate for solid propellant combustion usage.

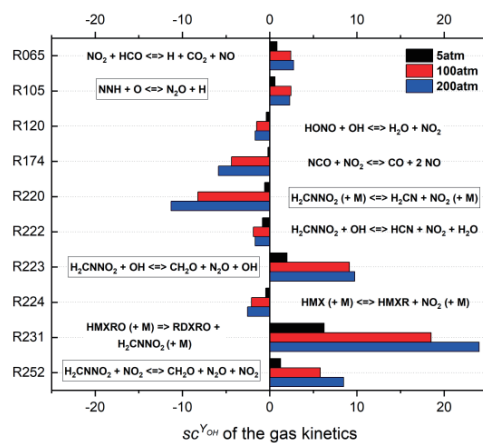


Fig. 7. Normalized sensitivity coefficients of gas kinetics to the ignition time (1500 K).

3.3 Sensitivity analysis of thermodynamics

Analogously to the kinetics parameters, the normalized sensitivity coefficients of c_p , h_f , and s of thermodynamic parameters under different pressures were calculated, and the top 10 sensitive parameters are presented (Fig. 8).

The results show that the r of HMX is strongly affected by the c_p of small molecules, such as H_2O , HCN, and CO. The most sensitive species was found to be H_2O with sc of c_p of -1.27 at 5 atm, which is around 10 times higher than the sc of the most sensitive gas kinetics (R220). It indicates that the thermodynamics of small species are 10 times more sensitive to the r of HMX than the gas kinetics. For species with negative sc of c_p (H_2O , CO, NO, N_2 , NH_3 , HCN), their molar concentration accounted for over 85 % (5 atm) in the HMX flame. It could explain their importance in the combustion process by

1
2
3
4
5
6
7
8
9
10
11
12
13
14
15
16
17
18
19
20
21
22
23
24
25
26
27
28
29
30
31
32
33
34
35
36
37
38
39
40
41
42
43
44
45
46
47
48
49
50
51
52
53
54
55
56
57
58
59
60
61
62
63
64
65

determining the heat feedback to the burning surface. While for species with positive sc (H, NNH, NCN, INT250a), their lifespans are short, and their concentrations are low. Thus, their main effect comes from their importance for the equilibrium constants of corresponding elementary reactions, which eventually determine reverse rate constants. The significance of their c_p values would further increase with pressure, indicating a stronger effect at a higher pressure, since the flame stand-off distance would be pressed with pressure. In addition, the significance of gas thermodynamic parameters on r is decreased in c_p , s , and h in sequence. The H radical has the highest sc of s under 100 atm (0.23), and the N_2 owns the most sensitive property of h_f (-0.02 at 5 atm), with a less important effect on r . Except for the c_p of liquid HMX, the sc' of liquid thermodynamic parameters are near zero (thus the results of liquid s are not presented). The sc of c_p of HMX was calculated to be 0.32 at 5 atm and it increases with pressures.

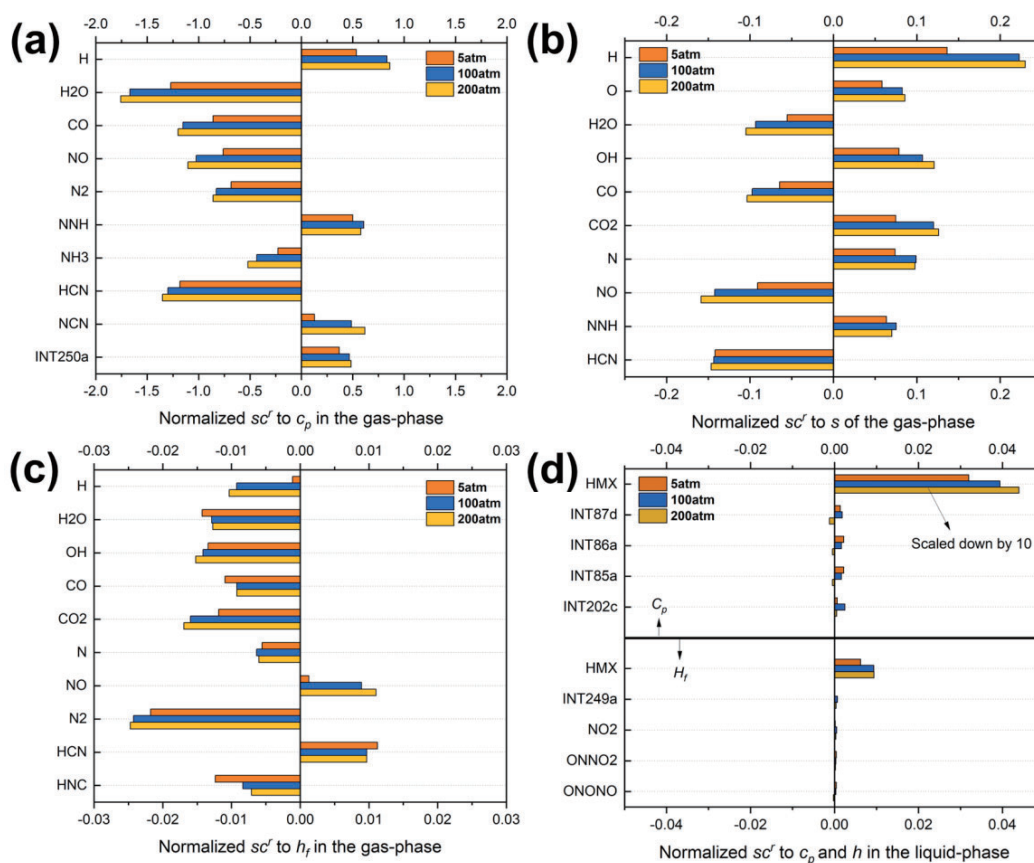


Fig. 8. Normalized sensitivity coefficients of gas thermodynamics: c_p (a), s (b), h_f (c) and liquid thermodynamics: c_p and h_f (d) to the r under different pressures.

3.4 Sensitivity analysis of transport

Since the mass diffusion in the liquid phase is ignored, only the sensitivity of gaseous species was investigated (Fig. 9). The collision diameter (σ) of small molecules (e.g. H₂O, H₂, CO) have high absolute sensitivity coefficients. Among them, the σ of H₂O is found to be the most sensitive one with sc of -0.158 at 5 atm, whose absolute value is higher than that of most sensitive gas kinetics (-0.13 of R220) at 5 atm.

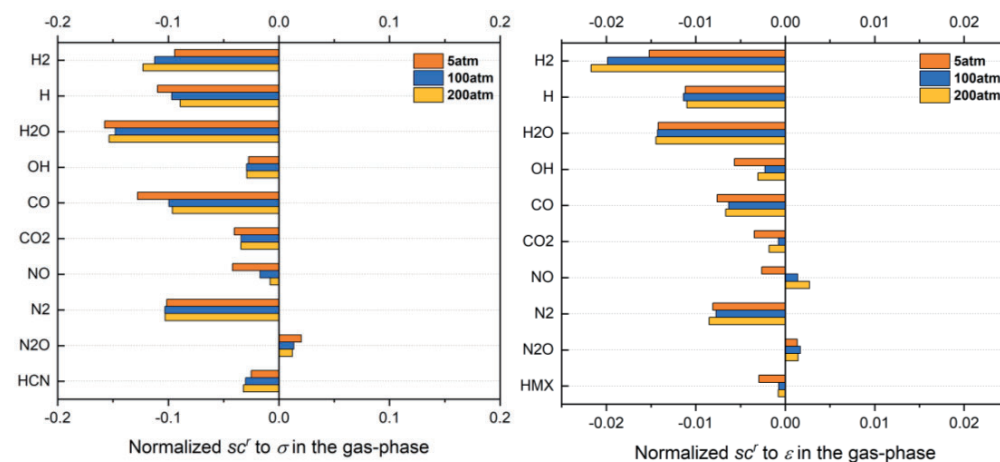


Fig. 9. Normalized sensitivity coefficients of collision diameters (σ) and potential well-depth (ε) of gaseous species to r under different pressures.

According to Patidar and Thynell's findings [42], the σ of RDX was identified to be the most sensitive transport parameter to the combustion of RDX. However, in this study, the σ of HMX ranked only 11th at 5 atm, which is assumed to be caused by the different methods to calculate the sensitivity coefficients. In Patidar et al.'s study [42], the target of the sensitivity analysis was chosen to be the temperature at the second grid point above the burning surface, where the initial species (HMX in this study) has a relatively higher concentration, which we assume to be the reason for leading to an overestimate of its significance. Similar species are ranked out with the most 10 sensitive potential well-depth (ε) as the results of σ , except for the HMX. It could be found that the ε exhibits less significance than the σ on r , which was assumed to be caused by the $1/\sigma^2$ dependence of σ with the transport properties, and the indirect relationship between the ε with collision integrals.

3.5. Normalized sensitivity coefficients

To further understand the role played by these parameters in HMX combustion, all calculated normalized sensitivity coefficients are summarized together, and the top 30 sensitive parameters at different pressures are selected (Fig. 10).

1
2
3
4
5
6
7
8
9
10
11
12
13
14
15
16
17
18
19
20
21
22
23
24
25
26
27
28
29
30
31
32
33
34
35
36
37
38
39
40
41
42
43
44
45
46
47
48
49
50
51
52
53
54
55
56
57
58
59
60
61
62
63
64
65

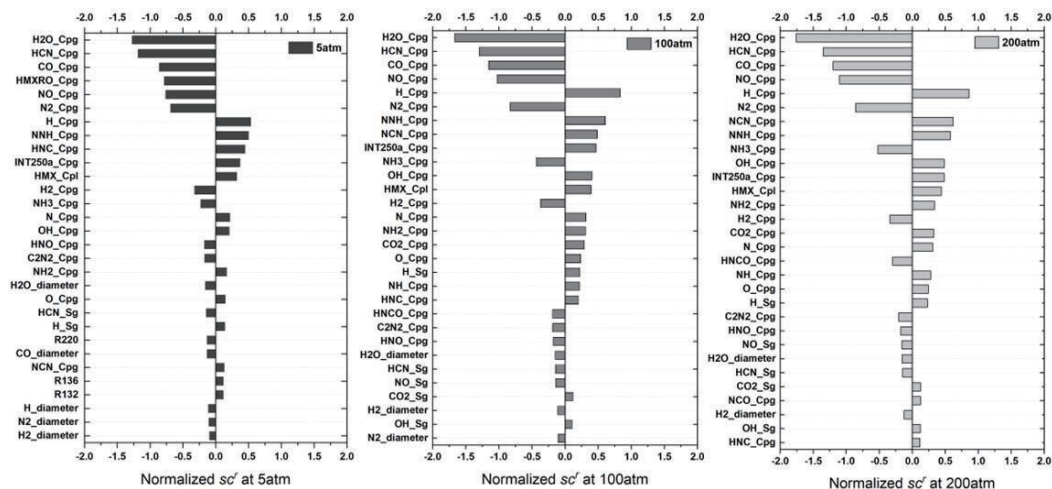


Fig. 10. Top30 mechanism parameters to r of HMX under different pressures.

It can be found that c_p of gaseous H_2O , HCN, and CO exhibit the highest sensitivities under all examined conditions, indicating that they influence the combustion of HMX most among all involved mechanism parameters. Their coefficients would further increase as pressure, and c_p of gaseous H_2O would reach -1.76 at 200 atm. The c_p of gaseous HMXRO has a high ranking at 5 atm, but it drops out of the top 30 under higher pressures. Overall, the c_p parameters of small gaseous species will dominate the combustion process, and more specifically, they would prohibit the regression of the burning surface. It could be assumed that the combustion process of HMX is controlled by the temperature gradient in the gas phase, as higher c_p requires more heat to achieve the same temperature gradient. The c_p of liquid HMX is the only selected parameter in the ranking out of the liquid mechanism. It indicates that the significance of the liquid mechanism is not comparable to the gas mechanism for HMX combustion, even under low pressures (e.g. 5 atm). Except for the c_p , the s and σ of small gaseous species are also significant, for instance, the s of gaseous HCN and H, and the σ of H_2O . Surprisingly, gas kinetics are not the most important factors in HMX combustion, especially when compared with thermodynamics at higher pressures. For instance, the gaseous decomposition of $H_2C_2N_2O_2$ (R220), R136, and R132 rank in the top 30 under 5 atm, but they disappear under 100 atm and 200 atm in the rankings. However, it is noted that the thermodynamic parameters of these small gaseous species with high sensitivities are quite known, leaving the gas kinetics to be the focus for the mechanism development. HMX as an exemplified case is representative enough to illustrate the combustion characteristics of energetic materials.

4. Conclusion

In this study, a comprehensive sensitivity analysis of kinetic, thermodynamic, and transport parameters in HMX combustion was performed by employing a one-dimensional steady-state numerical model that could accurately predict the combustion characteristics of HMX. The normalized sensitivity coefficients of all mechanism parameters were calculated under low, medium, and high pressures by the brute-force approach, and the significant parameters were identified and analyzed. The following major conclusions were drawn:

1. The results demonstrated that gas kinetics have a more significant impact on HMX combustion than liquid kinetics. Notably, the decomposition and isomerization reactions of H_2CNNO_2 are identified as the most sensitive in affecting r . Furthermore, the decomposition reaction of N_2O is found to have the largest effect on n of the HMX propellant.

2. The c_p of gaseous H_2O and HCN significantly influence the r of HMX, more than any other mechanism parameters. The liquid thermodynamic properties are not decisive in this respect, particularly under higher pressures.

3. It was found that the collision diameters of smaller species, such as HCN and H_2O , play a crucial role in HMX combustion. However, the effects of their potential well-depths are relatively negligible.

This research performed a comprehensive sensitivity analysis for detailed mechanisms in HMX combustion modeling. This approach not only aids in enhancing understanding of HMX combustion, guiding further improvement in the accuracy of HMX mechanisms through experiments and higher level theoretical calculations, but also highlights the focus on further developing, optimizing, and reducing the detailed kinetic mechanisms of solid propellants.

Declaration of competing interest

The authors declare that they have no known competing financial interests or personal relationships that could have appeared to influence the work reported in this paper.

Acknowledgment

We would like to express our sincere gratitude to the Dean's Chair fund at the National University of Singapore (WBS No. E-465-00-0010-02) and the High-Performance Computing of NUS for their support. We also acknowledge the National Research Foundation (NRF) under the Prime Minister's Office, Singapore, for their support through the Campus for Research Excellence and Technological Enterprise (CREATE) Programme (A00053280300).

Supplementary materials

The calculated burning rates, flame temperatures, and pressure exponents of HMX combustion under 5 atm, 100 atm, and 200 atm, together with the used HMX mechanism are provided in the Supplementary Materials.

REFERENCES

- [1] T.B. Brill, Connecting the chemical composition of a material to its combustion characteristics, *Prog. Energy Combust. Sci.* 18 (1992) 91-116.
- [2] R.A. Yetter, G.A. Risha, S.F. Son, Metal particle combustion and nanotechnology, *Proc. Combust. Inst.* 32 (2009) 1819-1838.
- [3] Q.-L. Yan, F.-Q. Zhao, K.K. Kuo, X.-H. Zhang, S. Zeman, L.T. DeLuca, Catalytic effects of nano additives on decomposition and combustion of RDX-, HMX-, and AP-based energetic compositions, *Prog. Energy Combust. Sci.* 57 (2016) 75-136.
- [4] G. Gupta, L. Jawale, D. Mehilal, B. Bhattacharya, Various methods for the determination of the burning rates of solid propellants: an overview, *Cent. Eur. J. Energ. Mat.* 12 (2015) 593-620.
- [5] J.-Y. Lyu, S.-L. Yang, S. Wu, G. Tang, W. Yang, Q.-L. Yan, Burning rate modulation for composite propellants by interfacial control of Al@AP with precise catalysis of CuO, *Combust. Flame* 240 (2022) 112029.
- [6] V. Radhakrishna, R.J. Tancin, G. Mathews, C.S. Goldenstein, Single-shot, mid-infrared ultrafast-laser-absorption-spectroscopy measurements of temperature, CO, NO and H₂O in HMX combustion gases, *Appl. Phys. B* 127 (12) (2021) 172.

- 1
2
3
4
5
6
7
8
9
10
11
12
13
14
15
16
17
18
19
20
21
22
23
24
25
26
27
28
29
30
31
32
33
34
35
36
37
38
39
40
41
42
43
44
45
46
47
48
49
50
51
52
53
54
55
56
57
58
59
60
61
62
63
64
65
- [7] P. Bernigaud, D. Davidenko, L. Catoire, A revised model of ammonium perchlorate combustion with detailed kinetics, *Combust. Flame* 255 (2023) 112891.
- [8] D. Chakraborty, R.P. Muller, S. Dasgupta, W.A. Goddard A, A detailed model for the decomposition of nitramines: RDX and HMX, *J. Comput. Aided Mater. Des.* 8 (2001) 203-212.
- [9] J.C. Park, D; Lin, Ming-Chang, Thermal decomposition of gaseous ammonium dinitramide at low pressure: kinetic modeling of product formation with ab initio MO/cVRRKM calculations, *Proc. Combust. Inst.* 27 (1998) 2351-2357.
- [10] J. Glorian, J. Ehrhardt, B. Baschung, Estimating ignition delay times of nitroglycerin: A chemical kinetic modeling study, *Combust. Sci. Technol.* 196, 3 (2024) 406-420.
- [11] J. Ehrhardt, J. Glorian, L. Courty, B. Baschung, P. Gillard, Detailed kinetic mechanism for nitrocellulose low temperature decomposition, *Combust. Flame* 258 (2023) 113057.
- [12] J.-Y. Lyu, Q. Zhu, X. Bai, X. Ren, J. Li, D. Chen, V.G. Kiselev, Y. Li, W. Yang, A detailed chemical kinetic mechanism of 1, 1-diamino-2, 2-dinitroethylene (FOX-7) initial decomposition in the gas phase, *Combust. Flame* 255 (2023) 112877.
- [13] V.G. Kiselev, N.P. Gritsan, Unexpected primary reactions for thermolysis of 1,1-diamino-2,2-dinitroethylene (FOX-7) revealed by ab initio calculations, *J. Phys. Chem. A.* 118 (2014) 8002-8008.
- [14] Y. Luo, C. Kang, R. Kaiser, R. Sun, The potential energy profile of the decomposition of 1,1-diamino-2,2-dinitroethylene (FOX-7) in the gas phase, *Phys. Chem. Chem. Phys.* (2022) 26836-26847.
- [15] B.E. Krisyuk, T.M. Sypko, Mechanism of thermolysis of hydrazino-dinitroethylenes, *Comput. Theor. Chem.* 1211 (2022) 113662.
- [16] L.-L. Liu, S.-Q. Hu, Ab initio calculations of the NO₂ fission for CL-20 conformers, *J. Energ. Mater.* 37 (2019) 154-161.
- [17] M.A. Kumar, P. Ashutosh, A.A. Vargeese, Decomposition mechanism of hexanitrohexaazaisowurtzitane (CL-20) by coupled computational and experimental study, *J. Phys. Chem. A.* 123 (2019) 4014-4020.
- [18] J. Zeng, L. Cao, M. Xu, T. Zhu, J.Z.H. Zhang, Complex reaction processes in combustion unraveled by neural network-based molecular dynamics simulation, *Nat. Commun.* 11 (1) (2020) 5713.
- [19] S. Cagnina, P. Rotureau, G. Fayet, C. Adamo, The ammonium nitrate and its mechanism of decomposition in the gas phase: a theoretical study and a DFT benchmark, *Phys. Chem. Chem. Phys.* 15 (2013) 10849.
- [20] Q. Chu, X. Chang, K. Ma, X. Fu, D. Chen, Revealing the thermal decomposition mechanism of RDX crystals by a neural network potential, *Phys. Chem. Chem. Phys.* 24 (2022) 25885-25894.
- [21] X. Chen, C.F. Goldsmith, Predictive kinetics for the thermal decomposition of RDX, *Proc. Combust. Inst.* 37 (2019) 3167-3173.
- [22] Z. Zhang, L. Ye, X. Wang, X. Wu, W. Gao, J. Li, M. Bi, Unraveling the reaction mechanism on pyrolysis of 1, 3, 5-trinitro-1, 3, 5-triazinane (RDX), *Combust. Flame* 242 (2022) 112220.
- 21

- 1 [23] L. Ye, Z. Zhang, F. Wang, X. Wang, Y. Lu, L. Zhang, Reaction mechanism and kinetic modeling of gas-phase
2 thermal decomposition of prototype nitramine compound HMX, *Combust. Flame* 259 (2024) 113181.
- 3 [24] R. Zhu, M.C. Lin, A complete quantum chemical prediction for reactions in three phases, *Aerosp. Tec. Japan* 10
4 (2012) 77-84.
- 5 [25] M. Khichar, L. Patidar, S.T. Thynell, Improvement and validation of a detailed reaction mechanism for thermal
6 decomposition of RDX in liquid phase, *Combust. Flame* 198 (2018) 455-465.
- 7 [26] L. Patidar, M. Khichar, S.T. Thynell, Identification of initial decomposition reactions in liquid-phase HMX
8 using quantum mechanics calculations, *Combust. Flame* 188 (2018) 170-179.
- 9 [27] A.S. Tomlin, The role of sensitivity and uncertainty analysis in combustion modelling, *Proc. Combust. Inst.* 34
10 (2013) 159-176.
- 11 [28] F. vom Lehn, L. Cai, H. Pitsch, Sensitivity analysis, uncertainty quantification, and optimization for
12 thermochemical properties in chemical kinetic combustion models, *Proc. Combust. Inst.* 37 (2019) 771-779.
- 13 [29] H.J. Curran, Developing detailed chemical kinetic mechanisms for fuel combustion, *Proc. Combust. Inst.* 37
14 (2019) 57-81.
- 15 [30] M.W. Beckstead, K. Puduppakkam, P. Thakre, V. Yang, Modeling of combustion and ignition of solid-propellant
16 ingredients, *Prog. Energy Combust. Sci.* 33 (2007) 497-551.
- 17 [31] T.L. Jackson, Modeling of Heterogeneous Propellant Combustion: A Survey, *AIAA J.* 50 (2012) 993-1006.
- 18 [32] C.F. Melius, Thermochemical modeling: II. Application to ignition and combustion of energetic materials, *Chem.*
19 *Phys. Energ. Mat.* (1990) 51-78.
- 20 [33] C.F. Melius, The thermochemistry and reaction pathways of energetic material decomposition and combustion,
21 *Philos. Trans. R. Soc. Lond. A* 339 (1992) 365-376.
- 22 [34] Y.-C. Liau, V. Yang, Analysis of RDX monopropellant combustion with two-phase subsurface reactions, *J.*
23 *Propul. Power.* 11 (1995) 729-739.
- 24 [35] R.A. Yetter, F.L. Dryer, M.T. Allen, J.L. Gatto, Development of gas-phase reaction mechanisms for nitramine
25 combustion, *J. Propul. Power.* 11 (1995) 683-697.
- 26 [36] J.E. Davidson, M. Beckstead, A three-phase model of HMX combustion, *Proc. Combust. Inst.* 26 (1996) 1989-
27 1996.
- 28 [37] E. Kim, V. Yang, Y.-C. Liau, Modeling of HMX/GAP pseudo-propellant combustion, *Combust. Flame.* 131
29 (2002) 227-245.
- 30 [38] M.S. Miller, W.R. Anderson, Burning-rate predictor for multi-ingredient propellants: nitrate-ester propellants,
31 *J. Propul. Power.* 20 (2004) 440-454.
- 32 [39] W.R. Anderson, C.B. Conner, Comparison of gas-phase mechanisms applied to RDX combustion model, *Proc.*
33 *Combust. Inst.* 32 (2009) 2123-2130.

- 1
2
3
4
5
6
7
8
9
10
11
12
13
14
15
16
17
18
19
20
21
22
23
24
25
26
27
28
29
30
31
32
33
34
35
36
37
38
39
40
41
42
43
44
45
46
47
48
49
50
51
52
53
54
55
56
57
58
59
60
61
62
63
64
65
- [40] K. Prasad, R.A. Yetter, M.D. Smooke, An Eigenvalue Method for Computing the Burning Rates of RDX Propellants, *Combust. Sci. Technol.* 124 (1997) 35-82.
- [41] D. Chakraborty, R.P. Muller, S. Dasgupta, W.A. Goddard, The mechanism for unimolecular decomposition of RDX (1,3,5-trinitro-1,3,5-triazine), an ab initio study, *J. Phys. Chem. A.* 104 (2000) 2261-2272.
- [42] L. Patidar, M. Khichar, S.T. Thynell, Intermolecular potential parameters for transport property modeling of energetic organic molecules, *Combust. Flame.* 200 (2019) 232-241.
- [43] L. Patidar, M. Khichar, S. Thynell, Modeling of HMX monopropellant combustion with detailed condensed-phase kinetics, *AIAA Propulsion and Energy 2019 Forum* 2019.
- [44] K. Prasad, R.A. Yetter, M.D. Smooke, An eigenvalue method for computing the burning rates of HMX propellants, *Combust. Flame* 115 (1998) 406-416.
- [45] P. Soni, C. Sarkar, R. Tewari, T.D. Sharma, HMX Polymorphs: Gamma to Beta Phase Transformation, *J. Energ. Mater.* 29 (2011) 261-279.
- [46] M.W. Beckstead, R.L. Derr, C.F. Price, A model of composite solid-propellant combustion based on multiple flames. *AIAA Journal*, 12 (1970) 2200-2207.
- [47] A. Zenin, HMX and RDX-Combustion mechanism and influence on modern double-base propellant combustion, *J. Propul. Power* 11 (1995) 752-758.
- [48] D.G. Goodwin, H.K. Moffat, I. Schoegl, R.L. Speth, B.W. Weber, Cantera: An object-oriented software toolkit for chemical kinetics, thermodynamics, and transport processes, 2023 Version 3.0.0.
- [49] D. Chakraborty, R.P. Muller, S. Dasgupta, W.A. Goddard, Mechanism for unimolecular decomposition of HMX (1, 3, 5, 7-tetranitro-1, 3, 5, 7-tetrazocine), an ab initio study, *J. Phys. Chem. A.* 105 (2001) 1302-1314.
- [50] L. Patidar, Thermal Decomposition and Combustion of RDX and HMX: Thermolysis Experiments and Molecular Modeling, PhD thesis, The Pennsylvania State University 2019.
- [51] M. Lemke, L. Cai, J. Reiss, H. Pitsch, J. Sesterhenn, Adjoint-based sensitivity analysis of quantities of interest of complex combustion models, *Combust. Theor. Model.* 23 (2019) 180-196.
- [52] N.J. Brown, K.L. Revzan, Comparative sensitivity analysis of transport properties and reaction rate coefficients, *Int. J. Chem. Kinet.* 37 (2005) 538-553.
- [53] S. F. Son, H.L. Berghout, C. A. Bolme, D. E. Chavez, D. Naud, M. A. Hiskey, Burn rate measurements of HMX, TATB, DHT, DAAF, and BTATz, *Proc. Combust. Inst.* 28 (2000) 919-924.
- [54] A.I. Atwood, T.L. Boggs, P.O. Curran, T.P. Parr, D.M. Hanson-Parr, C.F. Price, J. Wiknich, Burning Rate of Solid Propellant Ingredients, Part 1: Pressure and Initial Temperature Effects, *J. Propul. Power* 15 (1999) 740-747.
- [55] V. P. Sinditskii, M. V. Berezin, V. V. Serushkin, Mechanism of HMX combustion in a wide range of pressures, *Combust. Explos. Shock Waves* 45 (2009) 461-477.
- [56] A.A. Zenin, S.V. Finjakov, Studying RDX and HMX combustion mechanisms by various experimental techniques, *Combust. Explos. Shock Waves* 45 (2009) 559-578.

[57] A.A. Paletsky, E.N. Volkov, O.P. Korobeinichev, HMX flame structure for combustion in air at a pressure of 1 atm, *Combust. Explos. Shock Waves* 44 (2008) 639-654.

[58] M.E. DESIGNS, Chemkin-Pro, Ansys 2011.

1
2
3
4
5
6
7
8
9
10
11
12
13
14
15
16
17
18
19
20
21
22
23
24
25
26
27
28
29
30
31
32
33
34
35
36
37
38
39
40
41
42
43
44
45
46
47
48
49
50
51
52
53
54
55
56
57
58
59
60
61
62
63
64
65